

Ordered Ga wires formed on Si(100)- $2\times n$: Scanning tunneling microscopy study

Jun-Zhong Wang,¹ Jin-Feng Jia,¹ Xi Liu,¹ Wei-De Chen,¹ and Qi-Kun Xue,^{1,2,*}

¹State Key Laboratory for Surface Physics, Institute of Physics, The Chinese Academy of Sciences, Beijing 100080, China

²International Center for Quantum Structures, The Chinese Academy of Sciences, China

(Received 13 December 2001; published 24 May 2002)

Using the nanostructured Si(100)- $2\times n$ surface as a template, we have obtained large-scale well-aligned Ga nanowire arrays. High-resolution scanning tunneling microscopy (STM) images reveal that the deposited Ga atoms adsorb predominantly on top of the Si(100)- 2×1 dimer rows and form a stable local 2×2 structure so as effectively to remove Si dangling bonds states and saturate all Ga electron valency, a vital step that leads to the success of the method. An interesting observation is the formation of antiphase boundaries on the 2×2 -Ga phase. In this case, zigzag patterns were observed in the filled-state STM images, which provides further evidence for the parallel dimer model of the 2×2 -Ga reconstruction proposed previously.

DOI: 10.1103/PhysRevB.65.235303

PACS number(s): 68.65.La, 68.37.Ef, 68.35.Bs

I. INTRODUCTION

In the past decade, low-dimensional nanostructures have attracted great interest due to the potential to build up new optoelectronic and microelectronic devices. Atomic-scale wires, composed of several atom rows, could have different transport behavior from that in the bulk, due to distinct quantum effects. The group-III metals (Al, Ga, or In) on Si(100) are particularly interesting systems in terms of their characteristic one-dimensional anisotropic growth.¹⁻⁵ Deposited metal atoms grow much faster in the direction normal to the Si dimer rows, arranging themselves into various wires with different spacings. Using *ab initio* techniques, Brocks, Kelly, and Car¹ put forward a anisotropic accommodation mechanism, i.e., surface polymerization reaction, where the adatom has a strong preference to bond to the radical end of a dimer chain and becomes the new reactive site to continue the reaction. In addition, a total energy calculation indicates that,² under thermodynamic equilibrium conditions, group-III metal wires on Si(100) have a maximum length of na_0 [$a_0 = 3.84$ Å is the lattice constant in the (001) plane], with $n = 15, 18,$ and 14 for Al, Ga, and In, respectively. The spatial distribution of these wires on the surface is irregular and difficult to control. The limited length and nonuniform spacing of these wires is one of the major barriers for their applications. Meanwhile, other factors such as kinetics and surface defects can alter growth and the dimensions of the wires. Roland and Gilmer³ performed a molecular-dynamics study of Ge on a Si(100)- $2\times n$ surface; an additional diffusion barrier of 0.76 eV was found near the dimer vacancy lines (DVL's) to confine the adatom motion along the Si dimer rows. Therefore, we expect that, for group-III metals on the Si(100)- $2\times n$ surface, the diffusion anisotropy along and across the DVL's, as well as high-density surface defects, could significantly change the growth shape of the wires. In this sense, this nanostructured surface might be a tempting template for growing long atomic-scale wires to solve the above problem, as demonstrated with water-terminated Si(100)- $2\times n$ by Kida *et al.*⁴ and by ourselves.⁵

In general, the group-III metals on a Si(100)- 2×1 surface form several ordered phases at coverages less than 0.5 monolayer (ML) (1 ML = 6.8×10^{14} atoms/cm²). Most

studies have focused on the 2×2 phase by using low-energy electron diffraction (LEED),^{6,7} angle-resolved photoelectron spectroscopy,⁸⁻¹⁰ x-ray standing-wave measurements,^{11,12} and total energy calculations,^{1,13} as well as scanning tunneling microscopy (STM) for Al,^{14,15} Ga,¹⁶⁻¹⁹ and In,²⁰⁻²⁵ respectively. So far, it is widely accepted that the 2×2 phase can be best explained by the parallel dimer model, where the ad-dimers are centered at the valley bridge sites between the Si dimer rows with the Ga dimers oriented parallel to the underlying Si dimer bonds.^{11,23} In the empty-state STM images, the ad-dimer locations can be easily identified due to the large spatial extension of the empty p_z orbitals with π -type bondings toward the tip. However, the resolution is not sufficient to distinguish the orientation of the ad-dimers. On the other hand, for the filled states, owing to the poor spatial orbital extension of the highest occupied σ -type bonding state lying too close to the atomic cores, STM only shows a faint contrast for the ad-dimers. Recently, Evans and Nogami obtained very-high-resolution filled-state STM images for In and Ga on Si(100)- 2×1 ,²⁴ with a fairly good agreement with the simulated images.¹ However, up to now, of all the STM images reported, there is no direct evidence to distinguish between the parallel and orthogonal ad-dimer models. In the present paper, we report on the growth of well-aligned Ga wires on the Si(100)- $2\times n$ substrate and find convincing experimental evidence supporting the parallel ad-dimer model of the Ga-induced 2×2 reconstruction.

II. EXPERIMENT

The experiments were performed on a commercial Omicron ultrahigh-vacuum (UHV) variable-temperature STM, equipped with a LEED-Auger spectrometer with a base pressure of 5.0×10^{-11} mbar. Ga atomic beams were produced from an effusion cell with a standard boron nitride crucible. The STM images were obtained in the constant-current mode with electrochemically etched W tips. The samples used were heavily P-doped Si (001) wafers with a resistivity of ~ 0.001 Ω cm and were intentionally contacted to a stainless steel tweezer before loaded into the UHV system. The details of preparation of the Si(100)- $2\times n$ surface have been reported elsewhere.^{5,26} Ga was deposited to the as-prepared 2

$\times n$ surface at room temperature (RT) at a rate of ~ 0.06 ML per minute. A more accurate estimation of the Ga coverage was made by counting Ga ad-dimers observed in the STM images.

III. RESULTS AND DISCUSSION

The Si(100)- $2\times n$ surface has been studied by many groups since it was observed by Muller *et al.*²⁶ A tiny amount of metal contaminations, especially Ni contamination, can lead the dimer vacancies on the Si(100) surface to coalesce into DVL's.^{27,28} The n -fold ordering is driven by a short-range attractive interaction between vacancies in adjacent dimer rows and by a long-range repulsive interaction between vacancies in the same row.^{29,30} Zandvliet *et al.*³¹ have shown that the long-range repulsive interaction is related to strain relaxation. Since different numbers of dimers are missing in the vacancies, the vacancy lines are not straight.

Figure 1(a) shows a large-scale STM image of the as-prepared $2\times n$ surface. Here n varies from 8 to 12, depending on the annealing temperature and Ni impurity content. The structure is characterized by the DVL's (dark trenches) perpendicular to the dimer rows. Between the vacancy lines is the normal Si(100)- 2×1 dimer row structure shown as the bright stripes. The DVL's pervade the whole surface with good spatial periodicity.

Shown in Fig. 1(b) is an empty-state STM image after 0.1 ML Ga was deposited on the $2\times n$ surface at RT. The deposited Ga atoms predominantly occupy the normal 2×1 dimer rows, forming one-dimensional wires (the bright lines in the image) perpendicular to the Si dimer rows. Each line is composed of regularly spaced bright spots with a separation of $2a_0$ along the lines. At this coverage, along the $[0\bar{1}1]$ direction, the Ga wires have not connected with each other.

When the coverage increases to 0.25 ML, a well-ordered array of the Ga wires is formed. As shown in Fig. 2(a), most Ga wires are composed of two bright protrusion rows. From the high-resolution image shown in Fig. 2(b), the distance between the adjacent two lines along the $[011]$ direction is $2a_0$, indicating a local 2×2 ordering. Compared to the case on Si(100)- 2×1 , the Ga wires are very long, essentially extend from one step to the other of a terrace, and thus their lengths are simply determined by terrace sizes.

As for the formation mechanism of these wires, there are three possible causes: anisotropic diffusion, anisotropic adatom interaction, and anisotropic 2D accommodation coefficient. For the group-III metals on Si(100)- 2×1 , according to Brocks *et al.*¹ the activation energy for diffusion is small for both principal directions on the Si(100) surface (0.1 and 0.3 eV for diffusions of parallel and normal to the Si dimer row directions, respectively). This result suggests that at RT the mobility of adatoms is high in all directions, and the formation of wires can be attributed to the anisotropic accommodation coefficient, rather than the anisotropic diffusion. However, in the case of Si(100)- $2\times n$, in terms of the stability of the 2×2 Ga dimer structure (Ga atoms do not bond to Si atoms in DVL's), there is an anisotropic diffusion barrier due to the formation of steps at the DVL's, and an

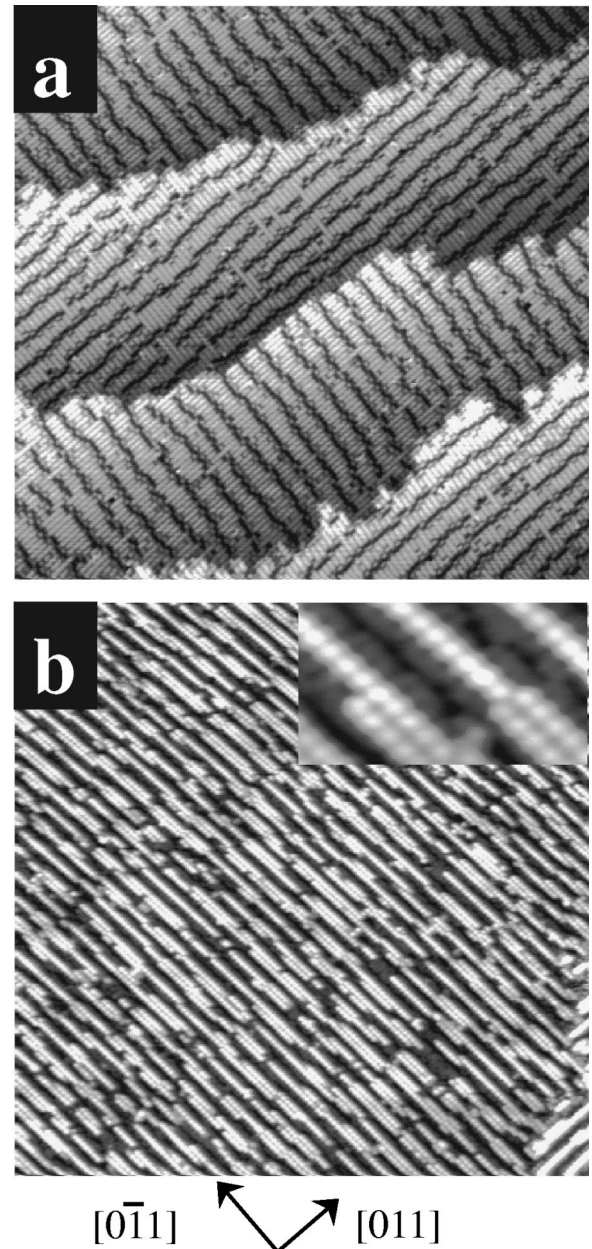


FIG. 1. (a) Typical STM image of an as-prepared Si(100)- $2\times n$ surface (100×100 nm², $V_s = -2.0$ V). (b) Empty-state STM image (100×100 nm², $V_s = +1.97$ V) of the Si(100)- $2\times n$ surface covered by 0.1 ML Ga; the inset is a closeup of the Ga wires.

atom has to overcome a barrier in order to diffuse cross the DVL's.³ Thus, the diffusion normal to the Si dimer row should be suppressed significantly; the probability for adatoms to occupy the regions between the DVL's to form the 2×2 structure is much higher. So an interplay between the anisotropic diffusion and anisotropic accommodation is responsible for the observed array of longer Ga wires.

In Fig. 2(b), we can clearly resolve both Ga and underlying Si. The Ga dimer protrusions are found to be located above the shallow minimum of the Si(100), which corresponds to the valley bridge site between the Si dimer rows according to recent STM studies.^{32,33} Meanwhile, we find that the dimer protrusions in Ga- 2×3 domains (indicated by

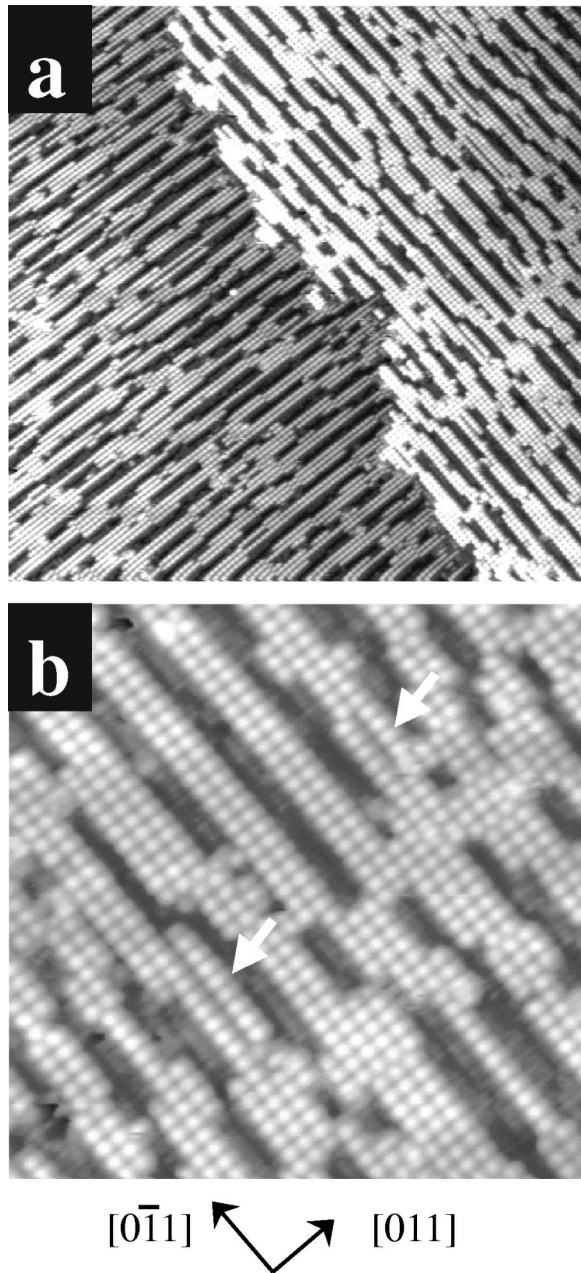


FIG. 2. Empty-state STM images of the Si(100)-2× n surface covered by 0.25 ML Ga. (a) Large-scale image ($100 \times 100 \text{ nm}^2$, $V_s = 1.85 \text{ V}$). (b) High-resolution image ($30 \times 30 \text{ nm}^2$, $V_s = 1.85 \text{ V}$); the 2×3 -Ga phase is indicated by the white arrow.

arrows) have a larger extension along the Si dimer row direction than that in the Ga- 2×2 domains. Previously, at high bias (+1.2 V), Itoh *et al.*¹⁵ observed Al dimer protrusions to be located above the deep minimum of Si(100)- 2×1 , which means that the Al dimer is located at the pedestal site of the Si dimer row, not consistent with the parallel dimer model.

Figure 3 shows a filled-state STM image of the same surface as shown in Fig. 2. The underlying Si dimer rows are clearly resolved. Some surplus Ga atoms appear brighter than the 2×2 Ga dimers. As the bias of -1.54 V lies in the binding energies of 1.0–1.5 and 1.5–2.0 eV for Ga-Si

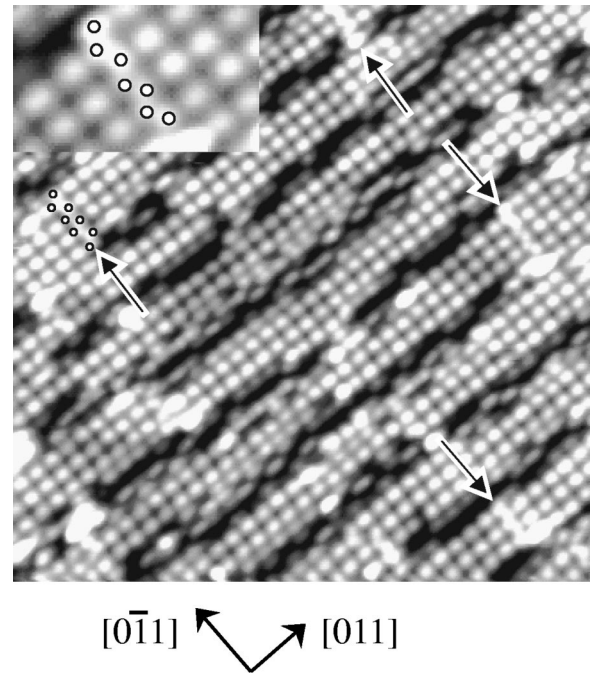


FIG. 3. Filled-state STM image ($30 \times 30 \text{ nm}^2$, $V_s = -1.54 \text{ V}$) of the same surface shown in Fig. 2. The antiphase boundaries on the 2×2 -Ga phase are indicated by the arrows. The insert is a close up STM image of an antiphase boundary.

backbonds,^{8,19} we speculate that the observed protrusions result mainly from the Ga-Si backbonds. Although the formation of the 2×2 Ga phase could eliminate both the surface dangling bonds and the surface states associated with the π bonds of Si dimers, the σ -bonding states of the Si dimers may be still visible.¹⁰ As a consequence, the protrusions in this image result from tunneling from both Ga-Si backbonds and the Si-Si dimer bonds.

An important observation here is the formation of antiphase domain boundaries, as indicated by the arrows in Fig. 3. At the antiphase boundary, the protrusions for the Ga dimers have a π phase shift. It is well known that the DVL's are not straight due to different numbers of the missed Si dimers. The resulting 2×1 domains have no uniform widths consisting of either even or odd numbers of Si dimers. When Ga dimers nucleate at the neighboring two Si dimer rows and these two Si rows have, respectively, odd and even missing Si dimers at DVL's, two Ga- 2×2 domains separated by the boundary between these two Si rows will be antiphased. The Ga dimer protrusions are elongated along the direction of the Ga dimer lines, perpendicular to that in the empty-state images. Although we have clearly determined the location of the Ga dimers from the high-resolution empty-state images, it is difficult to distinguish the orientation of the Ga dimers, whether parallel or orthogonal to the Si dimers.

However, by analyzing the structure of antiphase boundaries appearing in this filled-state image, we can discern the orientation of the Ga dimers. In Fig. 3, the protrusions form a zigzagged pattern at the antiphase boundary, and small round protrusions appear at each apex of the zigzags, with a separation of a_0 along the boundary. Such patterns, never

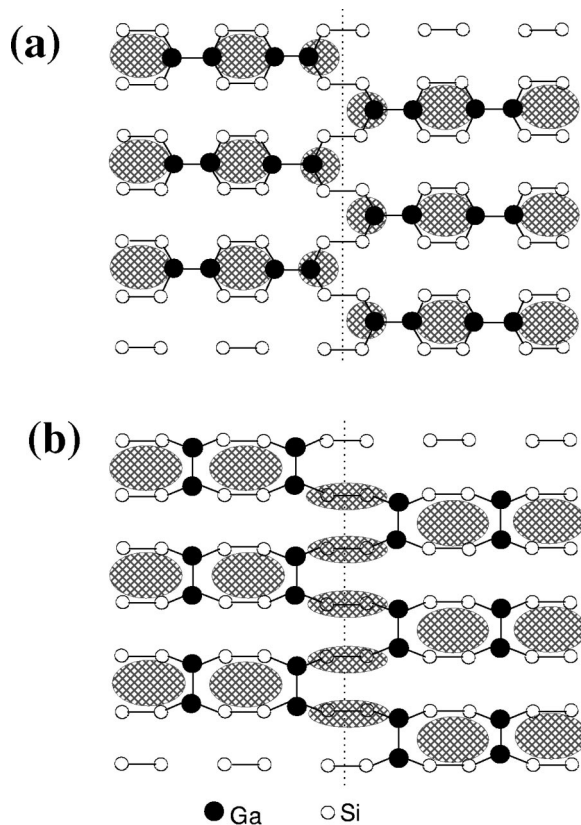


FIG. 4. Schematic illustration of the atomic structures of the antiphase boundaries based on the parallel dimer model (a) and the orthogonal dimer model (b). The solid circle denotes the Ga atom, the open one the Si atom. The hatched regions correspond to protrusions in the STM images.

observed in the Ga- 2×2 formed on the Si(100)- 2×1 , can be explained by the parallel dimer model shown in Fig. 4(a). The large round protrusions in the Ga dimer wires can be discerned as the rings associated with four Si-Ga bonds and two Si-Si dimers. At the boundary, owing to the missing of a

Ga atom from the rings, the protrusion shifts toward the remaining Ga atom, with the spatial extension decreased correspondingly. Such small protrusions can be located at both sides of the boundary, leading to a zigzagged pattern as schematically shown in Fig. 4(a). On the other hand, such a zigzagged pattern cannot be established from the orthogonal dimer model as displayed in Fig. 4(b), where the location of the protrusions is indicated by the hatched ellipses. Each large round protrusion in the lines involves four Ga-Si bonds and two Si-Si bonds. At the end of the lines, each protrusion will split into double-lobbed maxima with a striped shape. Each lobbed maximum corresponds to two Si-Ga bonds and a Si-Si bond. As a result, there should be a straight protrusion chain centered at the Si-Si dimer rows and parallel to the boundary. However, such a straight chain has never been observed in filled-state STM images. Therefore, the observed zigzagged protrusions at the antiphase boundary provide important evidence for the parallel dimer model, and the orthogonal dimer model can be ruled out.

IV. CONCLUSION

In summary, using a Si(100)- $2 \times n$ template, we have obtained large-scale well-aligned Ga wires perpendicular to the Si dimer rows. These wires predominantly occupy the normal 2×1 dimer row domain to establish a local stable 2×2 structure at a coverage of 0.25 ML. The Ga wires can be as long as 100 nm, simply determined by the terrace sizes of the $2 \times n$. The empty-state images clearly resolve the Ga dimers to be located in the valley bridge site between two Si dimer rows. In the filled-state images, we have observed a zigzagged pattern at the antiphase 2×2 domain boundary, which provides important evidence for the parallel ad-dimer model.

ACKNOWLEDGMENTS

This work is supported by the Natural Science Foundation of China under Grant Nos. 69625608 and 60076009.

*Electronic address: qkxue@aphy.iphy.ac.cn

¹G. Brocks, P.J. Kelly, and R. Car, Phys. Rev. Lett. **70**, 2786 (1993).

²Noboru Takeuchi, Phys. Rev. B **63**, 035311 (2001).

³C. Roland and G.H. Gilmer, Phys. Rev. B **47**, 16 286 (1993).

⁴A. Kida, H. Kajiyama, S. Heike, T. Hashizume, and K. Koike, Appl. Phys. Lett. **75**, 540 (1999).

⁵Jian-Long. Li, Xue-Jin. Liang, Jin-Feng. Jia, Xi. Liu, Jun-Zhong. Wang, En-Ge. Wang, and Qi-Kun. Xue, Appl. Phys. Lett. **79**, 2826 (2001).

⁶H. Sakama, K.I. Murakami, K. Nishikata, and A. Kawazu, Phys. Rev. B **48**, 5278 (1993); **50**, 14 977 (1994); **53**, 1080 (1996).

⁷R. Zhao, J.F. Jia, and W.S. Yang, Surf. Sci. Lett. **274**, L519 (1992).

⁸Y. Enta, S. Suzuki, and S. Kono, Surf. Sci. **242**, 277 (1991).

⁹H.W. Yeom, T. Abukawa, Y. Takakuwa, M. Nakamura, M. Kimura, A. Kakizaki, and S. Kono, Surf. Sci. **321**, L117 (1994).

¹⁰H.W. Yeom, T. Abukawa, Y. Takakuwa, Y. Mori, T. Shimatani, A.

Kakizaki, and S. Kono, Phys. Rev. B **53**, 1948 (1996).

¹¹Y. Qian, M.J. Bedzyk, S. Tang, A.J. Freeman, and G.E. Franklin, Phys. Rev. Lett. **73**, 1521 (1994).

¹²S. Tang, A.J. Freeman, Y. Qian, G.E. Franklin, and M.J. Bedzyk, Phys. Rev. B **51**, 1593 (1995).

¹³J.E. Northrup, M.C. Schabel, C.J. Karlsson, and R.I.G. Uhrberg, Phys. Rev. B **44**, 13 799 (1991).

¹⁴J. Nogami, A.A. Baski, and C.F. Quate, Phys. Rev. B **44**, 1415 (1991).

¹⁵H. Itoh, J. Itoh, A. Schmid, and T. Ichinokawa, Phys. Rev. B **48**, 14 663 (1993).

¹⁶A.A. Baski, J. Nogami, and C.F. Quate, J. Vac. Sci. Technol. A **8**, 245 (1990).

¹⁷J. Nogami, S.-I. Park, and C.F. Quate, Appl. Phys. Lett. **53**, 2086 (1988).

¹⁸J. Nogami, A.A. Baski, and C.F. Quate, J. Vac. Sci. Technol. A **8**, 3520 (1990).

¹⁹H. Sakama, A. Kawazu, T. Sueyoshi, T. Sato, and M. Iwatsuki,

- Phys. Rev. B **54**, 8756 (1996).
- ²⁰J. Knall, J.-E. Sundgen, G.V. Hansson, and J.E. Greene, Surf. Sci. **166**, 512 (1986).
- ²¹A.A. Baski, J. Nogami, and C.F. Quate, Phys. Rev. B **43**, 9316 (1991).
- ²²A.A. Baski, J. Nogami, and C.F. Quate, J. Vac. Sci. Technol. A **9**, 1946 (1991).
- ²³B.E. Steele, Lian Li, J.L. Stevens, and I.S.T. Tsong, Phys. Rev. B **47**, 9925 (1993).
- ²⁴M.M.R. Evans and J. Nogami, Phys. Rev. B **59**, 7644 (1999).
- ²⁵Z.-C. Dong, D. Fujita, and H. Nejoh, Phys. Rev. B **63**, 115402 (2001).
- ²⁶K. Muller, E. Lang, L. Hammer, W. Grimm, P. Heilman, and K. Heinz, in *Determination of Surface Structure by LEED*, edited by P.M. Marcus and F. Jona (Plenum, New York, 1984), p. 483.
- ²⁷H. Niehus, U.K. Köhler, M. Copel, and J.E. Demuth, J. Microsc. **152**, 735 (1988).
- ²⁸K. Kato, T. Ide, S. Miura, A. Tamura, and T. Ichinokawa, Surf. Sci. **194**, L87 (1988).
- ²⁹P.C. Weakliem, Z. Zhang, and H. Metiu, Surf. Sci. **336**, 303 (1995).
- ³⁰Fu-Kwo Men, Arthur R. Smith, Kuo-Jen Chao, Zhenyu Zhang, and Chih-Kang Shih, Phys. Rev. B **52**, R8650 (1995).
- ³¹H.J.W. Zandvliet, H.K. Louwsma, P.E. Hegeman, and Bene Poelsema, Phys. Rev. Lett. **75**, 3890 (1995).
- ³²X.R. Qin and M.G. Lagally, Phys. Rev. B **59**, 7293 (1999).
- ³³Kenji Hata, Satoshi Yasuda, and Hidemi Shigekawa, Phys. Rev. B **60**, 8164 (1999).